Cooperative effects of Rho and mechanical stretch on stress fiber organization

Roland Kaunas*†‡, Phu Nguyen*†, Shunichi Usami*†, and Shu Chien*†§¶

Departments of *Bioengineering and §Medicine and †The Whitaker Institute of Biomedical Engineering, University of California at San Diego, La Jolla, CA 92093

Contributed by Shu Chien, September 21, 2005

The small GTPase Rho regulates the formation of actin stress fibers in adherent cells through activation of its effector proteins Rho-kinase and mDia. We found in bovine aortic endothelial cells that inhibitions of Rho, Rho-kinase, and mDia (with C3, Y27632, and F1F2Δ1, respectively) suppressed stress fiber formation, but fibers appeared after 10% cyclic uniaxial stretch (1-Hz frequency). In contrast to the predominately perpendicular alignment of stress fibers to the stretch direction in normal cells, the stress fibers in cells with Rho pathway inhibition became oriented parallel to the stretch direction. In cells with normal Rho activity, the extent of perpendicular orientation of stress fibers depended on the magnitude of stretch. Expressing active RhoV14 plasmid in these cells enhanced the stretch-induced stress fiber orientation by an extent equivalent to an additional ≈3% stretch. This augmentation of the stretch-induced perpendicular orientation by RhoV14 was blocked by Y27632 and by F1F2Δ1. Thus, the activity of the Rho pathway plays a critical role in determining both the direction and extent of stretch-induced stress fiber orientation in bovine aortic endothelial cells. Our results demonstrate that the stretch-induced stress fiber orientation is a function of the interplay between Rho pathway activity and the magnitude of stretching.

cytoskeletal dynamics | endothelial cells | mechanotransduction | Rho-kinase

The tension generated by contraction of adherent cells against their underlying surface results in an internal stress field that depends on the organization of the cytoskeleton and the associated adhesive contacts (see ref. 1 for review). Intracellular forces have an important role in cellular functions such as migration, proliferation, apoptosis, differentiation, and gene expression (see refs. 2–4 for reviews). Actin stress fibers, which are formed in response to cell contraction (5), consist of bundles of actin microfilaments cross-linked by α-actinin, myosin, myosin light-chain, tropomyosin, and other proteins arranged in a manner similar to that in muscle sarcomeres (6). Stress fibers represent the main contractile apparatus in non-muscle cells (7) and are the primary structures associated with intracellular tension. Stress fibers terminate at focal adhesions, which attach the cell to the extracellular matrix (8). Isometric contraction of a cell would result in tension development in the stress fibers, which are anchored at their ends.

The activation of the small GTPase Rho leads to stress fiber assembly (9) and cell contraction by means of myosin light chain phosphorylation (5), which is regulated by Rho-kinase, a downstream effector of Rho (10). mDia, another Rho effector, is also involved in stress fiber formation downstream of Rho activation (11), possibly by regulating actin polymerization and focal adhesion turnover through its association with profilin (12, 13) and src-tyrosine-kinase (14), respectively.

Cyclic uniaxial stretch induces the orientation of stress fibers in endothelial cells (ECs) perpendicular to the principal direction of stretch (15). The stretch-induced perpendicular orientation of EC stress fibers is blocked by inhibitors of Rho, Rho-kinase, or myosin light chain (MLC) activity, indicating the importance of the Rho/Rho-kinase/MLC pathway in this orientation (16–18). In airway smooth muscle cells, cyclic stretch can cause Rho activation, and an increased Rho activation due to lysophosphatidic acid can enhance cell orientation perpendicular to stretch (19). The effects of mDia on cell and stress fiber remodeling in response to cyclic stretch have not been reported.

No method exists for measuring the forces generated in stress fibers in living cells. Cell stiffness, which is closely related to cytoskeletal tension (20), has been shown to increase in response to mechanical stretch and cell contraction (20, 21). These results suggest that each of these stimuli can generate tension in stress fibers. Here, we sought to determine the roles of cyclic stretch and Rho-induced cell contractility on stress fiber organization and the underlying mechanisms. Rho activity was inhibited with C3 exoenzyme and enhanced with an active mutant of Rho (RhoV14). In addition, the roles of the Rho downstream effectors Rho-kinase and mDia in mediating the effects of Rho on stretch-induced stress fiber organization were assessed by inhibiting their activities. In the absence of stretch, stress fibers were randomly organized independent of the level of Rho activity. Cyclic uniaxial stretch induced the perpendicular orientation of stress fibers to an extent dependent on both the level of Rho activity and the magnitude of stretch. RhoV14 expression exerted an effect on the direction of stretch-induced stress fiber orientation equivalent to increasing the stretch magnitude by ≈3%. When the Rho pathway was inhibited, cyclic uniaxial stretch led to the formation of stress fibers oriented parallel, rather than perpendicular, to the direction of stretch. Therefore, the level of Rho activity modulates the extent and direction of orientation of stress fibers in stretched cells. These findings provide information on the mechanisms underlying stress fiber orientation and tension generation in ECs in response to uniaxial mechanical stretch and demonstrate the quantitative relations between Rho signaling and mechanical stretch in their cooperative effects on stress fiber organization.

Materials and Methods

Cell Culture. Bovine aortic endothelial cells (BAECs) were isolated from the aorta and cultured in DMEM (GIBCO/BRL) supplemented with 10% FBS, 2 mM L-glutamine, 1 mM penicillin-streptomycin, and 1 mM sodium pyruvate (22). Cell cultures and stretch experiments were performed in a humidified 95% air, 5% CO_2 incubator at 37°C.

Application of Mechanical Stretch. BAECs were subjected to 6 h of cyclic stretch (1–10% linear stretch) at a frequency of 1 Hz as described (23), with the stretch chamber and indenter geometries modified to produce cyclic uniaxial stretch (Fig. 1). This

Conflict of interest statement: No conflicts declared.

Abbreviations: EC, endothelial cell; BAEC, bovine aortic EC.

‡Present address: Department of Biomedical Engineering, Texas A & M University, College Station, TX 77843.

¶To whom correspondence should be addressed at: Powell-Focht Bioengineering Hall, Room 134, University of California at San Diego, La Jolla, CA 92093. E-mail: shuchien@ucsd.edu.

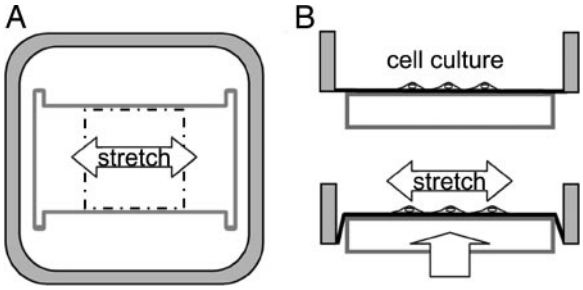

Fig. 1. Top (*A*) and side (*B*) views of a stretch chamber and indenter to illustrate the principle of cell stretching. An I-shaped teflon indenter pushed up against a silicone rubber membrane secured to a square frame results in a principal stretch oriented along the long axis of the indenter. The small tension generated in the orthogonal direction is opposed by the tendency for the membrane to compress orthogonal to the principal stretch direction. The extensions at the corners of the indenter increase the uniformity of the strain field over the indenter, resulting in a virtually uniaxial stretch. Cells were seeded in the central 4 × 4-cm region of the membrane where strain was uniform.

cyclic uniaxial stretch is referred to as "stretch" hereafter. The central region of the membrane, which was confined with the aid of a Teflon insert, was coated with 10 μg/ml fibronectin (Sigma) overnight and washed with sterile PBS. BAECs were seeded on the coated region of the membrane and allowed to spread overnight. For experiments on confluent cultures, the cells were seeded at ≈50% confluence and cultured for 2 more days to achieve confluence. Strains were measured by imaging the displacement of particles adhered to the central 4 × 4-cm surface of the membrane with a charge-coupled device (CCD) camera and microscope with a ×4 objective and by analyzing their displacements offline. Strains parallel and perpendicular to the principal stretch direction were 0.099 ± 0.008 and 0.005 ± 0.007, respectively (mean ± SD), thus resulting in essentially 10% uniaxial stretch.

Transfections and Chemical Inhibitors. Plasmids containing hemagglutinin (HA)-tagged RhoV14 and GFP-tagged C3 were obtained from M. Schwartz (University of Virginia, Charlottesville) (24, 25). Plasmids containing Myc-tagged pEF and F1F2Δ1 were obtained from R. Treisman (University College, London) (26). GFP was expressed in BAECs as pEGFP-C1 plasmid (Clontech). Transient transfections were performed on BAECs at ≈80% confluence with FuGENE 6 (Roche Diagnostics) in the presence of serum. Twenty-four hours later, the cells were trypsinized, seeded in the stretch chamber, and allowed to spread overnight before the stretch experiment. In experiments with C3 transfections, the culture media was removed, and confluent BAECs were transfected with 10 μg of C3 exoenzyme (Calbiochem) and 15 μl of Lipofectamine (GIBCO/BRL) per chamber in serum-free conditions for 3 h. Control cells were transfected with BSA. The cells were then incubated in their original culture media for 1 h before the stretch experiment. In experiments using Y27632 (10 μM, Calbiochem) to inhibit Rho-kinase activity (27), the cells were pretreated 30 min before stretch, and Y27632 was present throughout the experiment.

Cell Staining and Fluorescence Microscopy. After stretching, the cells were washed with PBS at 37°C, fixed in 4% paraformaldehyde in PBS for 10 min at room temperature, and permeabilized with 0.5% Triton X-100 in PBS for 15 min. Cells expressing GFP or GFP-C3 were identified by epifluorescence. To identify cells expressing myc-tagged pEF (empty vector of F1F2Δ1) or F1F2Δ1, the fixed cells were incubated with rabbit anti-myc antibody (Santa Cruz Biotechnology) for 1 h, washed with PBS, and incubated with fluorescein donkey anti-rabbit secondary antibody for 30 min. After washing cells with PBS, actin filaments were labeled with rhodamine-phalloidin (Molecular Probes) for 45 min. All labelings were performed at 1:200 dilution in PBS containing 1% BSA. Images were captured by using an imaging system, which included a spinning-disk confocal Olympus microscope with a ×60 objective, a Hamamatsu ORCA II ER cooled charge-coupled device (CCD)-camera (Hamamatsu Photonics, Hamamatsu City, Japan), and IPLAB imaging software (Scanalytics, Billerica, MA). All transfected cells (transfection efficiency ≈10%) were used for imaging and analysis; at least 25 transfected cells were collected for each condition.

Quantification of Stress Fiber Orientations in Nonconfluent Cells. We used an image processing algorithm based on pixel intensity gradients to quantify stress fiber orientation distributions within individual nonconfluent cells (28). The orientation of structures in 20 × 20-pixel subregions of an image was determined by computing the direction of minimal gradient in pixel intensity in each subregion. Subregions lacking highly stained features (i.e., without f-actin bundles) were ignored by excluding subregions having an average pixel intensity below a threshold value (0.4 × mean pixel intensity of entire image). Subregions containing neighboring cells were also excluded. From the orientation angles of the remaining subregions, a mean stress fiber orientation angle was computed for each image, i.e., each cell. The distributions of mean orientations are presented as circular histograms to illustrate the orientation of stress fibers relative to the stretch direction.

Statistical Analysis. Circular statistical analysis was performed, and histograms were plotted by using ORIANA 2 software (Kovach

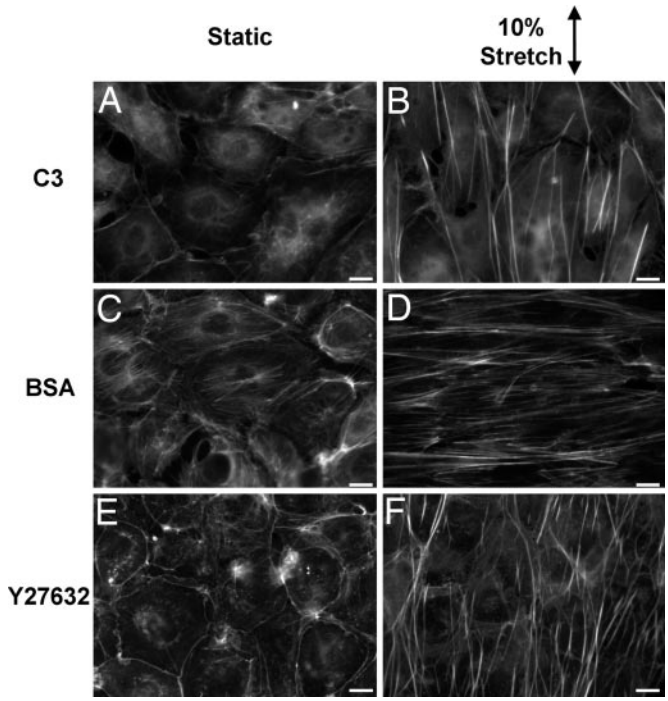

Fig. 2. Cooperative and interactive effects of Rho inhibition and cyclic uniaxial stretch on stress fiber orientation in BAECs. Representative micrographs are shown of confluent BAECs transfected with C3 (*A* and *B*) or BSA (*C* and *D*) or treated with Y27632 (*E* and *F*), and either kept as unstretched controls (*A*, *C*, and *E*) or subjected to 6 h of 10% cyclic stretch (*B*, *D*, and *F*). The cells were stained with rhodamine-phalloidin to identify f-actin bundles. BSA transfection served as a control for the effects of protein transfection. (Scale bars: 10 μm.)

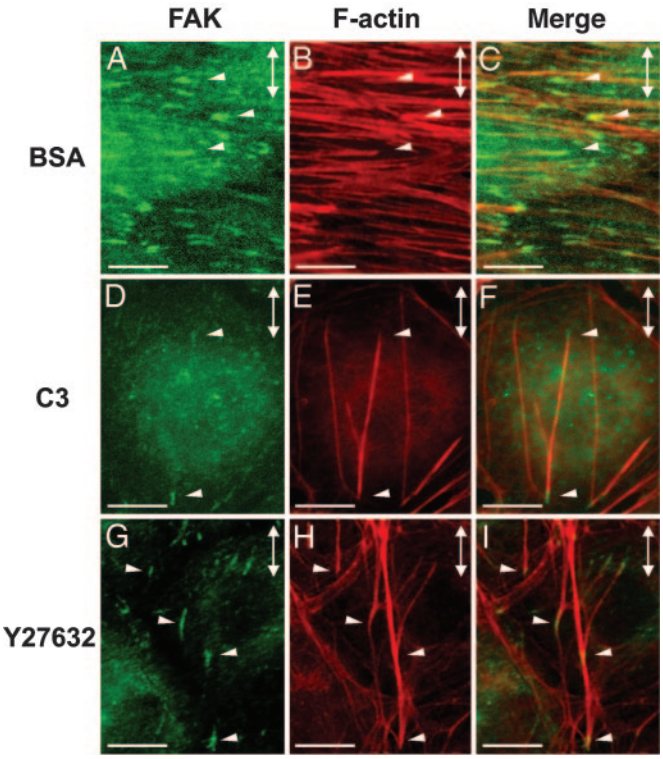

Fig. 3. Stretch-induced actin bundles are associated with focal adhesions. Representative micrographs of confluent BAECs transfected with BSA (*A–C*) or C3 (*D–F*), or treated with Y27632 (*G–I*), and subjected to 6 h of 10% cyclic stretch. The direction of stretch is shown by double-headed arrows in the upper right corner of each panel. The cells were double-stained with a focal adhesion kinase antibody (*A*, *D*, and *G*) to identify focal adhesions and rhodamine-phalloidin (*B*, *E*, and *H*) to identify f-actin bundles. The two images were superimposed (*C*, *F*, and *I*) to illustrate colocalization of actin bundles and focal adhesions (arrowheads). (Scale bars: 10 μm.)

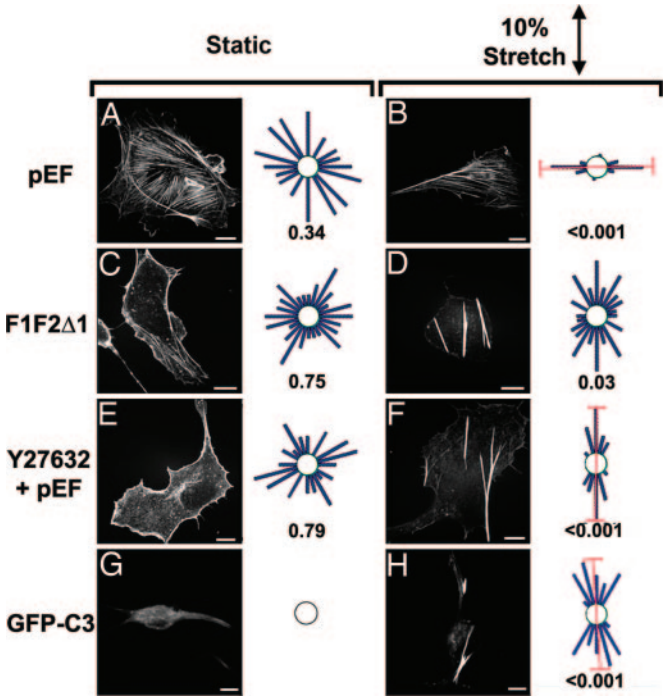

Fig. 4. Effects of inhibition of Rho-kinase or mDia on stretch-induced actin organization in sparsely seeded BAECs. Representative micrographs are shown for myc- or GFP-positive BAECs, which had been transfected with myc-pEF (*A* and *B*) or myc-F1F2Δ1 (*C* and *D*), transfected with myc-pEF and treated with 10 μM Y27632 (*E* and *F*), or transfected with GFP-C3 (*G* and *H*). For each condition, cells were kept as unstretched controls (*A*, *C*, *E*, and *G*) or subjected to 6 h of 10% cyclic stretch (*B*, *D*, *F*, and *H*). The distribution of mean stress fiber orientations for each condition is summarized in a circular histogram, with the data separated into 15° intervals. Because the orientation angles can be defined in either direction, the histogram bars are drawn symmetrically on opposite sides of the circle. *P* values indicate the significance of testing whether the distributions are different from a random distribution (Rayleigh test). Mean values and 99% confidence intervals are shown in red for distributions with $P < 0.01$.

Computing Services, Angelsey, Wales). The mean resultant length (R) was calculated as an indicator for the extent of stress fiber orientation. R is determined by vectorial summation of the individual orientation vector components and normalization by the total cell number (N_{cell}) using Eq. **1**,

$$R = \frac{1}{N_{\text{cell}}}\sqrt{\sum_{j=1}^{N_{\text{cell}}} \sin 2\theta_j + \sum_{j=1}^{N_{\text{cell}}} \cos 2\theta_j}, \qquad [1]$$

where θ_j is the angle for cell j. R is a measure of uniformity of orientation vector distribution, with values ranging from 0 to 1, corresponding to perfectly random and totally aligned distributions, respectively. The Rayleigh test was used to assess the degree of uniformity of distribution of axial vectors, i.e., whether the distribution has a significant direction. The Watson U^2 test was used to identify significant differences between axial vector distributions.

Results

Roles of Rho-Induced Contractility and Stretch in Stress Fiber Organization. In these experiments, we assessed the independent and cooperative effects of two modes of modulation of intracellular tension, i.e., Rho-induced contractility and uniaxial mechanical stretch, on stress fiber organization in confluent BAECs. In BAECs transfected with C3 exoenzyme to block contractility, stress fiber formation was almost completely absent under unstretched condition (Fig. 2*A*); 10% stretch at 1 Hz of these cells caused the formation of linear actin fiber bundles, which were oriented parallel to the direction of stretch (Fig. 2*B*). Unstretched BAECs transfected with BSA, which does not inhibit Rho activity, contained actin fibers not oriented in any particular direction (Fig. 2*C*). Stretching of these BSA-transfected cells resulted in the orientation of stress fibers perpendicular to the direction of stretch (Fig. 2*D*). Thus, whereas actin fiber formation can be induced independently by externally applied tension (Fig. 2 *B* vs. *A*) and Rho-induced contractility (Fig. 2 *C* vs. *A*), the orientation of these fibers resulting from the stretching of ECs with Rho activity present (Fig. 2*D*) is a function of their interactive effects. Immunostaining with an antibody specific for focal adhesion kinase (FAK) revealed the association of these fibers with focal adhesion-like structures in a manner similar to that of stress fibers both in the control cells transfected with BSA (Fig. 3*C*) and in cells transfected with C3 (Fig. 3*F*).

Effects of Inhibition of Rho-Kinase and mDia on Stretch-Induced Stress Fiber Organization. We next investigated the roles of downstream effectors of Rho, namely Rho-kinase and mDia, on stretch-induced stress fiber remodeling in confluent BAECs. Inhibition of Rho-kinase activity by Y27632 attenuated stress fiber formation in unstretched cells (Fig. 2*E*), and uniaxial stretch of Y27632-treated cells resulted in the formation of stress fibers parallel to stretch direction (Fig. 2*F*), which were associated with focal adhesion-like structures (Fig. 3*I*).

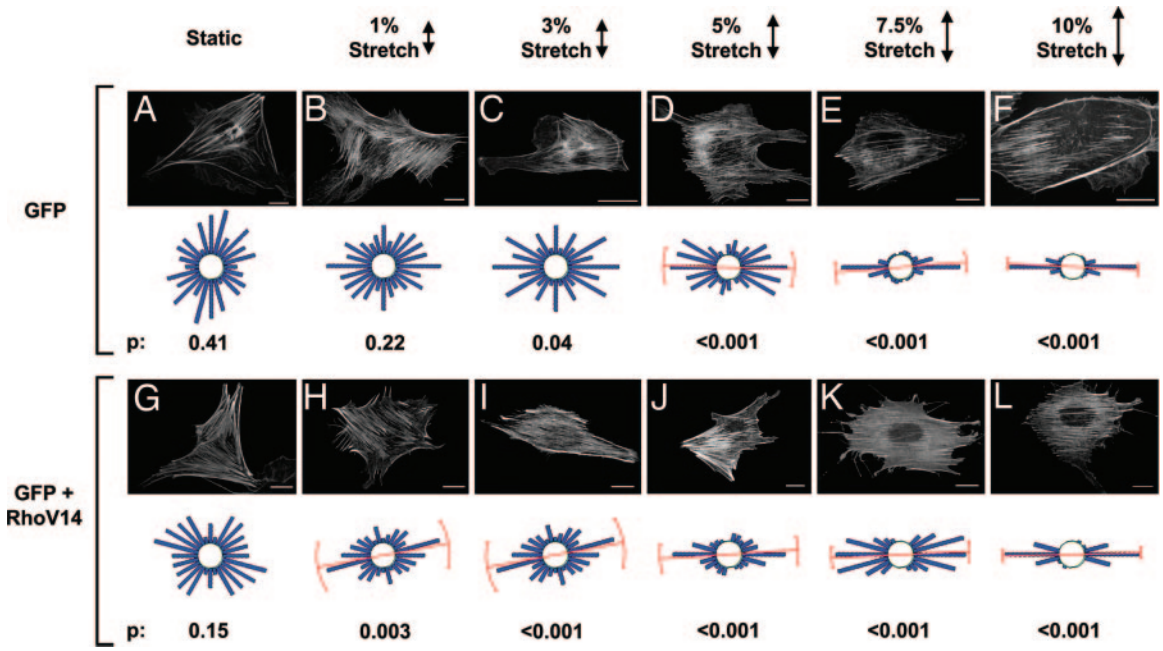

Fig. 5. Effects of stretch magnitude and RhoV14 expression on stress fiber orientation. Representative micrographs, circular histograms, and *P* values (Rayleigh test; as in Fig. 4) are shown for BAECs [expressing GFP alone (*A–F*) or coexpressing RhoV14 and GFP (*G–L*)] that were either kept as an unstretched controls (*A* and *G*) or subjected to cyclic stretch at 1% (*B* and *H*), 3% (*C* and *I*), 5% (*D* and *J*), 7.5% (*E* and *K*), or 10% (*F* and *L*) for 6 h.

Transfection of BAECs with a dominant-negative mutant of mDia, F1F2Δ1, which can inhibit lysophosphatidic acid-induced formation of stress fibers in NIH 3T3 cells (26) resulted in successful expression in ≈10% of cells; therefore, the cells were seeded sparsely to avoid the effects of neighboring untransfected cells on the transfected cells. Stress fibers in cells expressing the empty vector (pEF) were randomly oriented when unstretched (Fig. 4*A*), and they became oriented in the perpendicular direction when stretched (Fig. 4*B*). F1F2Δ1 expression led to a general suppression of stress fibers in unstretched cells (Fig. 4*C*), but stretch caused the formation of prominent stress fibers that were oriented in the parallel direction (Fig. 4*D*).

The results on the effects of C3 and Y27632 were obtained on confluent BAECs, whereas the studies with F1F2Δ1 were performed on sparsely seeded cells. To assess whether cell density had an influence, we tested the effects of C3 and Y27632 on sparsely seeded cells. Similar to the results observed with confluent BAECs (Fig. 2 *A*, *B*, *E*, and *F*), stretching of sparsely seeded C3-transfected or Y27632-treated cells (Fig. 4 *E–H*) induced the formation of stress fibers oriented in the parallel direction. Thus, the inhibition of either Rho-kinase or mDia, as with inhibition of Rho, resulted in the formation of stress fibers oriented parallel, rather than perpendicular, to the stretch direction.

RhoV14 Enhances Stress Fiber Orientation Perpendicular to the Direction of Stretch to an Extent Equivalent to ≈3% Stretch. We measured the magnitude dependence of stretch-induced stress fiber orientation in cells coexpressing the constitutively active mutant RhoV14 and GFP as compared with cells expressing GFP alone (Fig. 5). GFP-expressing cells did not show significant orientation of stress fibers when unstretched or subjected to 1% stretch (Fig. 5 *A* and *B*). The orientation of the stretch fibers to the direction of stretch was marginally significant at 3% stretch (Fig. 5*C*), and it became increasingly more uniform as the stretch magnitude was increased to 10% (Fig. 5 *D–F*). Coexpression of RhoV14 did not induce any significant orientation in the absence of stretch (Fig. 5*G*), as in the case of unstretched cells expressing GFP alone (Fig. 5*A*). The stress fibers in RhoV14-expressing BAECs showed significant perpendicular orientation at a stretch magnitude as low as 1% (Fig. 5*H*), and the orientation became more uniform as the stretch magnitude was increased to 10% (Fig. 5 G–L). This finding is noteworthy because neither RhoV14 in the absence of stretch nor 1% stretch in the absence of RhoV14 caused significant orientation in stress fibers. We analyzed these results to assess the effects of RhoV14 expression and stretch and their interplay on stress fiber orientation. The extent of stress fiber orientation, as measured by using the mean resultant length (*R*), increased with increasing stretch magnitude for both the cells expressing GFP and the cells coexpressing RhoV14/GFP (Fig. 6). Comparison between these groups at

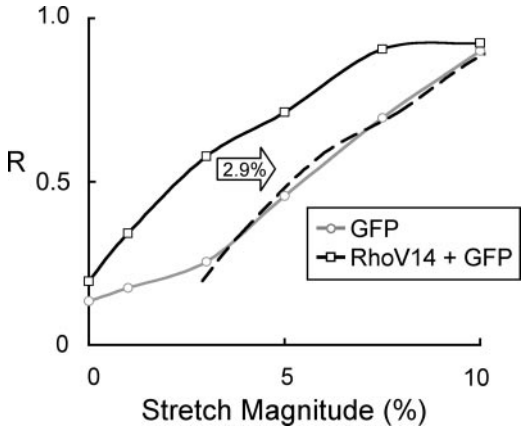

Fig. 6. RhoV14 expression is equivalent to the effect of an additional 2.9% stretch. The mean resultant length (*R*) for the various stretch magnitudes is plotted against stretch magnitude for BAECs expressing GFP alone (○) or coexpressing RhoV14 and GFP (□). Shifting the RhoV14/GFP curve to the right by 2.9% on the stretch axis (dashed curve) shows excellent agreement with the curve for GFP alone, indicating that the RhoV14 expression mimics the effects of an additional 2.9% stretch.

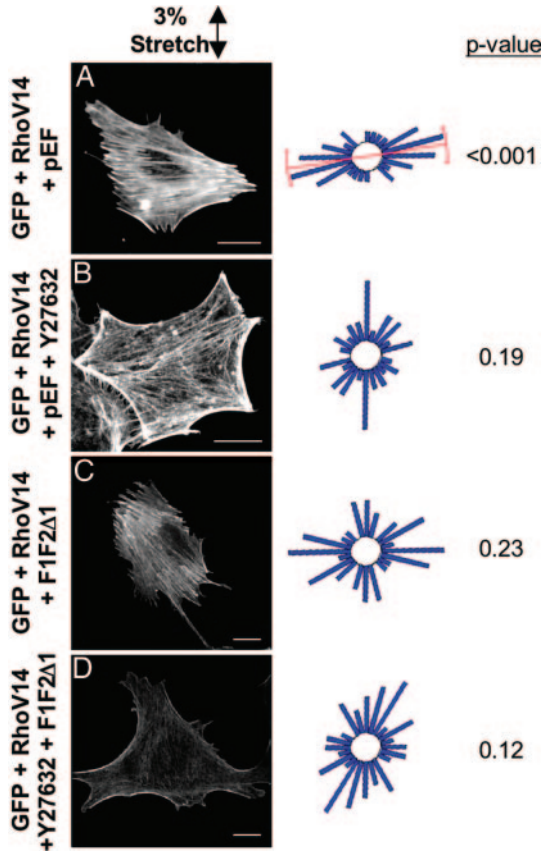

Fig. 7. Y27632 and F1F2Δ1 block the enhancement of stretch-induced cell orientation by RhoV14. Representative micrographs, circular histograms, and *P* values (Rayleigh test; as in Fig. 4) are shown for BAECs that had been transfected with RhoV14/GFP plus pEF (A), Y27632 (*B*), F1F2Δ1 (*C*), or a combination of Y27632 and F1F2Δ1 (*D*), and subjected to 6 h of 3% cyclic stretch.

given stretch magnitudes indicates that the *R* value for cells coexpressing RhoV14/GFP was higher than that for cells expressing GFP alone at all magnitudes except at 10% stretch, at which point both curves approach a maximal value near unity. Given the parallel nature of the two curves along the *x* axis, it is instructive to compare the stretch magnitude required to achieve a given *R* value. Such comparison shows that the RhoV14/GFP requires 2.9% less stretch to attain the same *R* value; i.e., shifting the RhoV14/GFP curve to the right by 2.9% stretch results in an excellent agreement with the curve for GFP alone.

Inhibitions of Rho-Kinase and mDia Block the Effects of RhoV14 on Stretch-Induced Stress Fiber Orientation. To elucidate the mechanism by which RhoV14 increased stress fiber orientation, we tested whether Y27632 or F1F2Δ1 would block the perpendicular orientation of stress fibers in response to the combined treatment of RhoV14 and 3% stretch. The 3% stretch was chosen because this is the magnitude at which RhoV14/GFP cells and GFP-only cells showed the greatest and statistically most significant difference in stress fiber orientation (Fig. 6). The stress fibers in cells coexpressing GFP/RhoV14 and pEF showed significant orientation perpendicular to 3% stretch (Fig. 7*A*). This perpendicular orientation was blocked by the additional treatment with Y27632 (Fig. 7*B*) or coexpression of F1F2Δ1 (Fig. 7*C*), as well as combination of Y27632 and F1F2Δ1 (Fig. 7*D*). These findings indicate that Rho-kinase and mDia activities are needed for the enhancement of stretch-induced perpendicular stress fiber orientation by RhoV14 expression.

Discussion

Cyclic uniaxial stretch can cause cells and their stress fibers to orient perpendicular to the direction of stretch in nonconfluent osteoblasts and fibroblasts (29), nonconfluent vascular smooth muscle cells (30), and confluent airway smooth muscle cells (31). It has been shown that stretch-induced perpendicular orientation of stress fibers in nonconfluent and confluent ECs requires Rho and Rho-kinase activity (16, 17). Our study has demonstrated that stretch is capable of inducing the formation of stress fibers and associated focal adhesions in the absence of Rho activity; importantly, these stress fibers are oriented parallel, rather than perpendicular, to the direction of stretch. These results were obtained by using different inhibitors of the Rho-signaling pathway, including the Rho inhibitor C3 exoenzyme, the Rho-kinase inhibitor Y26732, and the mDia dominant-negative mutant F1F2Δ1, and under both confluent and nonconfluent culture conditions. The application of automated measurement and statistical analysis to quantify the orientation of the stress fibers has provided further support to the conclusion that stress fibers are oriented parallel to the direction of stretch after inhibition of the Rho pathway. We have shown the cooperative effects of Rho activity and mechanical stretch, as well as their quantitative equivalence, in inducing the perpendicular orientation of stress fibers.

The mechanism by which stretch induces the formation and orientation of stress fibers in cells after inhibition of Rho activity is unclear. Other signaling molecules that have been shown to be involved in stretch-induced cell and stress fiber orientation include stretch-activated ion channels (32) and focal adhesion proteins such as focal adhesion kinase (33) and src (34). Because stress fiber formation due to Rho activity has been attributed to the generation of cytoskeletal tension (5), it is possible that stretch *per se* can increase the cytoskeletal tension to cause stress fiber formation. This finding is supported by our observation that stress fibers become preferentially oriented parallel to the direction of stretch-induced intracellular tension. Thus, whereas the Rho-signaling pathway is not essential for stress fiber formation in response to stretch, it is critical for the stretch-induced perpendicular orientation of stress fibers.

Our results show that the effects of Rho in the stretch-induced perpendicular orientation of stress fibers are mediated by both Rho-kinase and mDia. Treatment with inhibitors of either Rho-kinase or mDia caused the stress fibers to orient parallel to the direction of stretch in a pattern similar to that observed with a Rho inhibitor. In addition, inhibitors of Rho-kinase or mDia blocked the effects of RhoV14 on stretch-induced stress fiber orientation perpendicular to the direction of 3% stretch. Because expression of active mDia induces the formation of thin actin filament bundles and active Rho-kinase induces the formation of thick, condensed stress fibers (11), Rho-kinase is probably more important than mDia in inducing the formation of thick stress fibers. In our studies on cells expressing active RhoV14, Rho-kinase inhibition abolished most stress fibers with only thin fibers remaining (Fig. 7*B*), whereas mDia inhibition did not block stress fiber formation (Fig. 7*C*). Both Rho-kinase and mDia were necessary for the enhancement of stretch-induced stress fiber orientation (Fig. 7*A*); however, they seem to involve different processes.

The mechanism by which RhoV14 expression enhances the perpendicular orientation of stress fibers to stretch may be explained in terms of the combined effects of stretch and Rho activity on tension in stress fibers. A recent study by Costa *et al.* (35) indicates that individual stress fibers behave like prestressed one-dimensional elastic filaments. The findings that extension of isolated actin filaments can result in an increase in filament tension and that this effect is fully reversible upon release of the extending force (36, 37) are in

support of this hypothesis. Stretching the substrate upon which cells are adhered can increase tension in the actin cytoskeleton (21), and this stretching induces rapid disassembly of stress fibers oriented in the direction of stretch, followed by reassembly of stress fibers away from the stretch direction (30). This dynamic response has been suggested to relieve the excessive tension generated in stress fibers that are oriented in the stretch direction (38). Rho agonists have been shown to increase cell contractility (5). Thus, RhoV14 expression, by constitutively stimulating stress fiber contraction, may act to increase the basal level of tension in stress fibers. We found that RhoV14 expression is equivalent to an increase in the magnitude of stretch in inducing a given extent of perpendicular orientation, which, for BAECs subjected to stretch at 1 Hz, was equivalent to a 2.9% (or ≈3%) increase in stretch magnitude. It is possible that this value may be different for different frequencies of stretch, but the main point is that the chemical stimulation provided by increased Rho activity has an equivalence to the mechanical stimulation of uniaxial stretch in regulating stress fiber orientation. The present results provide support for our hypothesis that contractility and stretch cooperatively contribute to cytoskeletal tension. Furthermore, these results are consistent with the concept that the perpendicular orientation of stress fibers relieves the increase in tension generated by stretch, resulting in a more stable configuration for the actin cytoskeleton.

In summary, our results show that cyclic uniaxial stretch can induce stress fiber orientation by two different mechanisms, depending on the level of Rho activity. In the absence of signaling through the Rho pathway, stretch causes the formation of stress fibers oriented in the direction of stretch-induced tension. When the Rho signaling pathway is intact, however, stress fibers are oriented perpendicular to the direction of stretch-induced tension to an extent dependent on the level of Rho activity and the magnitude of stretch applied. An increase in Rho activity can reduce the magnitude of stretch required to achieve a given degree of perpendicular orientation of stress fibers. We propose that active orientation of the actin cytoskeleton mediated by Rho may represent a mechanism by which ECs reduce the increase in intracellular tension generated by cyclic stretching. Further, we propose that the basal level of intracellular tension, which is regulated by Rho, may determine the sensitivity of the cell to mechanical stretching.

Support for this research was provided by National Institutes of Health Grants HL 19454, HL 43026, and HL 64382. R.K. was a Whitaker Foundation graduate fellow and a trainee supported by National Institutes of Health Training Grant T32HL07089.

1. Galbraith, C. G. & Sheetz, M. P. (1998) *Curr. Opin. Cell Biol.* **10,** 566–571.
2. Chen, C. S., Tan, J. & Tien, J. (2004) *Annu. Rev. Biomed. Eng.* **6,** 275–302.
3. Hinz, B. & Gabbiani, G. (2003) *Curr. Opin. Biotechnol.* **14,** 538–546.
4. Chien, S., Li, S. & Shyy, Y. J. (1998) *Hypertension* **31,** 162–169.
5. Chrzanowska-Wodnicka, M. & Burridge, K. (1996) *J. Cell Biol.* **133,** 1403–1415.
6. Langanger, G., Moeremans, M., Daneels, G., Sobieszek, A., De Brabander, M. & De Mey, J. (1986) *J. Cell Biol.* **102,** 200–209.
7. Burridge, K. (1981) *Nature* **294,** 691–692.
8. Burridge, K., Fath, K., Kelly, T., Nuckolls, G. & Turner, C. (1988) *Annu. Rev. Cell Biol.* **4,** 487–525.
9. Ridley, A. J. & Hall, A. (1992) *Cell* **70,** 389–399.
10. Amano, M., Chihara, K., Kimura, K., Fukata, Y., Nakamura, N., Matsuura, Y. & Kaibuchi, K. (1997) *Science* **275,** 1308–1311.
11. Watanabe, N., Kato, T., Fujita, A., Ishizaki, T. & Narumiya, S. (1999) *Nat. Cell Biol.* **1,** 136–143.
12. Carlier, M. F. & Pantaloni, D. (1997) *J. Mol. Biol.* **269,** 459–467.
13. Schluter, K., Jockusch, B. M. & Rothkegel, M. (1997) *Biochim. Biophys. Acta* **1359,** 97–109.
14. Satoh, S. & Tominaga, T. (2001) *J. Biol. Chem.* **276,** 39290–39294.
15. Dartsch, P. C. & Betz, E. (1989) *Basic Res. Cardiol.* **84,** 268–281.
16. Yano, Y., Saito, Y., Narumiya, S. & Sumpio, B. E. (1996) *Biochem. Biophys. Res. Commun.* **224,** 508–515.
17. Birukov, K. G., Jacobson, J. R., Flores, A. A., Ye, S. Q., Birukova, A. A., Verin, A. D. & Garcia, J. G. (2003) *Am. J. Physiol.* **285,** L785–L797.
18. Wang, J. H., Goldschmidt-Clermont, P. & Yin, F. C. (2000) *Ann. Biomed. Eng.* **28,** 1165–1171.
19. Smith, P. G., Roy, C., Zhang, Y. N. & Chauduri, S. (2003) *Am. J. Respir. Cell Mol. Biol.* **28,** 436–442.
20. Wang, N., Tolic-Norrelykke, I. M., Chen, J., Mijailovich, S. M., Butler, J. P., Fredberg, J. J. & Stamenovic, D. (2002) *Am. J. Physiol.* **282,** C606–C616.
21. Pourati, J., Maniotis, A., Spiegel, D., Schaffer, J. L., Butler, J. P., Fredberg, J. J., Ingber, D. E., Stamenovic, D. & Wang, N. (1998) *Am. J. Physiol.* **274,** C1283–C1289.
22. Li, S., Kim, M., Hu, Y. L., Jalali, S., Schlaepfer, D. D., Hunter, T., Chien, S. & Shyy, J. Y. (1997) *J. Biol. Chem.* **272,** 30455–30462.
23. Sotoudeh, M., Jalali, S., Usami, S., Shyy, J. Y. & Chien, S. (1998) *Ann. Biomed. Eng.* **26,** 181–189.
24. Chong, L. D., Traynor-Kaplan, A., Bokoch, G. M. & Schwartz, M. A. (1994) *Cell* **79,** 507–513.
25. del Pozo, M. A., Vicente-Manzanares, M., Tejedor, R., Serrador, J. M. & Sanchez-Madrid, F. (1999) *Eur. J. Immunol.* **29,** 3609–3620.
26. Copeland, J. W. & Treisman, R. (2002) *Mol. Biol. Cell* **13,** 4088–4099.
27. Uehata, M., Ishizaki, T., Satoh, H., Ono, T., Kawahara, T., Morishita, T., Tamakawa, H., Yamagami, K., Inui, J., Maekawa, M. & Narumiya, S. (1997) *Nature* **389,** 990–994.
28. Karlon, W. J., Hsu, P.-P., Li, S., Chien, S., McCulloch, A. D. & Omens, J. H. (1999) *Ann. Biomed. Eng.* **27,** 712–720.
29. Neidlinger-Wilke, C., Grood, E. S., Wang, J. H-.C., Brand, R. A. & Claes, L. (2001) *J. Orthop. Res.* **19,** 286–293.
30. Hayakawa, K., Sato, N. & Obinata, T. (2001) *Exp. Cell Res.* **268,** 104–114.
31. Smith, P. G., Garcia, R. & Kogerman, L. (1997) *Exp. Cell Res.* **232,** 127–136.
32. Naruse, K., Yamada, T. & Sokabe, M. (1998) *Am. J. Physiol.* **274,** H1532–H1538.
33. Naruse, K., Yamada, T., Sai, X. R., Hamaguchi, M. & Sokabe, M. (1998) *Oncogene* **17,** 455–463.
34. Sai, X., Naruse, K. & Sokabe M. (1999) *J. Cell Sci.* **112,** 1365–1373.
35. Costa, K. D., Hucker, W. J. & Yin, F. C. (2002) *Cell Motil. Cytoskeleton* **52,** 266–274.
36. Kojima, H., Ishijima, A. & Yanagida, T. (1994) *Proc. Natl. Acad. Sci. USA* **91,** 12962–12966.
37. Liu, X. & Pollack, G. H. (2002) *Biophys. J.* **83,** 2705–2715.
38. Wang, J. H. (2000) *J. Theor. Biol.* **202,** 33–41.